



A path planning control for a vessel dynamic positioning system based on robust adaptive fuzzy strategy

X. K. Dang ^a, H. N. Truong^{a,b} and V. D. Do^{a,c}

^aGraduate School, Ho Chi Minh City University of Transport, Chi Minh, Vietnam; ^bManagement, Ba Ria - Vung Tau College of Technology, Vung Tau, Vietnam; ^cDongan Polytechnic, Vung Tau, Vietnam

ABSTRACT

The thrusters and propulsion propellers systems, as well as the operating situations, are all well-known nonlinearities which are caused less accuracy of the dynamic positioning system (DPS) of vessels in the path planning control process. In this study, to enhance the robust performance of the DPS, we proposed a robust adaptive fuzzy control model to reduce the effect of uncertainty problems and disturbances on the DPS. Firstly, the adaptive fuzzy controller with adaptive law is designed to adjust the membership function of the fuzzy controller to minimize the error in path planning control of the vessel. Secondly, the H_∞ performance of robust tracking is proved by the Lyapunov theory. Moreover, compared to the other controller, a simulation experiment comprising two case studies confirmed the efficiency of the approach. Finally, the results showed that the proposed controller reaches control quality, performance and stability.

ARTICLE HISTORY

Received 4 September 2021
Accepted 7 March 2022

KEYWORDS

Adaptive law; dynamic positioning system; membership function; path planning control; robust adaptive fuzzy

1. Introduction

Traditional support vessels have been employed during most of the drilling and exploration stages, with minimal use throughout the production stage. Drill rigs and offshore platforms need regular delivery of supplies that must be available at all times. Anchor handling tug supply, platform supply vessels and fast supply vessels are the formed offshore support vessels (OSVs) that fulfil this duty. However, the logistics support and transportation of products, tools, equipment and personnel to and from offshore oil platforms and other offshore structures are the key roles of most of these OSVs. A new generation of OSVs has developed in recent decades, most of which are arranged with a Class 1 or Class 2 dynamic positioning system (DPS) [1]. More importantly, the DPS assists the OSV in all of its responsibilities, including transit, survival and station maintenance, and the differences in required electrical systems for propulsion are significant. Thruster units generally range in power from a few hundred to a few more thousand hp, with four, six or eight variable-speed thruster designs, as well as control situations requiring the use of all thrusters. Moreover, the DPS is a control system among nonlinear properties because of their complex structure, diverse working conditions and high accuracy requirements under the influence of the going environment [2–4]. As a result, in the study of DPS, researchers are focused on two primary concerns: first, the control methods used to mitigate system disturbances and uncertainties, and second, enhanced the performance of the control process (Table 1).

Despite recent advancements in reducing system disturbances and uncertainties, the issues such as modelling uncertainties, environmental interferences and unmeasurable velocity remain partially achievable. To address the aforementioned issues, several studies have focused on DPS [5], such as nonlinear adaptive control [6], sliding mode control [7], back-stepping control [8] and the combination of two or more control techniques to cope with uncertainty disturbances and parameters. Recently, Sørensen [9], Dang et al. [10] and Wang et al. [11] surveyed a lot of previous research materials which introduce some modern control theories to aim at improving the quality of the DPS. Basically, the nonlinearity and uncertain disturbance must be taken in consideration while almost the traditional control theories are simple in structure and method, the disadvantages of these methods were that the kinetic functions of motions must be linearized under certain conditions. From the above, the modern theories, such as fuzzy logic control, neural network control (NNC), cerebellar model articulation control (CMAC), neural-fuzzy control (NFC) and adaptive neural-fuzzy robust position control scheme [12], deep learning-based semi-supervised control [13] has been widely investigated from different perspectives. To clarify the fundamental research issues, we analyse more carefully the control algorithms related to DPS in the next paragraphs.

In addition, the thruster fault-tolerant control [14] utilized the Luenberger observation to identify actuator abnormalities, and the DPS is offered by a discrete-time

Table 1. List of nomenclature.

Abbreviation	Description
DPS	Dynamic positioning system
OSVs	Offshore support vessels
FLC	Fuzzy logic control
NNC	Neural network control
CMAC	Cerebellar model articulation control
NFC	Neural-fuzzy control
TSF	Takagi–Sugeno fuzzy
RAFC	Robust adaptive fuzzy controller
AFC	Adaptive fuzzy controller
MFs	Membership functions

variable controller determined through the supervisor. Therefore, the DPS is guaranteed against nonlinearity induced by actuator failures, according to simulation tests conducted on a scale model of an offshore vessel. The limitation of this study is not examined in light of the impact of unanticipated elements on vessel motion, such as environmental and control process time delays effected. As a consequence, developing finite quadratic optimum controllers for DPS is a way simpler. So far, using an NNC to detect the wave amplitude and estimate the external force [15], which affects the vessel, simulation is applied to display dynamic position. However, a practical test is required to verify the suggested technique. In other solutions, the CMAC was based on the PID algorithm to approximate the nonlinear components to improve control quality [16], while the authors in [17] improved the resilience of the CMAC for the DPS. CMAC's responses suggest that the controller can adjust to external influences, even if the vessel moves at high speeds with uncertain parameters. In fact, the disadvantage of most of the above studies is mainly studying the stability of the controller while they have not mentioned or fully resolved the robustness of the system in different boundary conditions.

Related to enhance the performance of the DPS, the Takagi–Sugeno fuzzy (TSF) model design is an excellent approach for achieving the modelling and controlling of nonlinear systems, and sectors nonlinear and localized approximation are regularly utilized in the fuzzy inference system. Considering the fuzzy control for vessel maneuvering, in connectivity environments, a dynamic positioning controller model for an unmanned marine vehicle is of significance [18,19]. Moreover, by utilizing the yaw angle's variation scope as well as the sampler-to-controller and controller-to-actuator network-induced features, network-based TSF models for the DPS have been developed [20]. The trajectory tracking control issue of a dynamic positioning is investigated in [21], which is complicated by modelling uncertainties, environmental disturbances and unmeasurable velocity. A suitable stability criterion for the TSF controller is constructed and a less conservative solution is achieved by integrating the convex reciprocal inequalities and Lyapunov theorems. It can be seen that the fuzzy control by changing properties is

an effective solution in controlling nonlinear systems. Regarding reducing the influence of the environment, several methods related to fuzzy control, such as active disturbance rejection control [22,23] and approximated adaptive fuzzy control [24,25], which showed that disturbance rejections are the fairly common solutions in vessel motion control. Moreover, the DPS model using TSF is the appropriate option for the study of vessel maneuvering, especially in path planning control or routing control.

In several years, the nonlinear adaptive control approach has been investigated to cope with the difficulty of uncertainties and disturbances [2–4,26]. For the DPS control method, the stationary Kalman filter for the vessel positioning problem is approximately equivalent to a notch filter in cascade with a second filter [27]. An adaptive neural-fuzzy algorithm is studied to obtain the most suitable control parameters for thrust systems by overcoming environmental disturbances [26]. Moreover, an output-feedback nonlinear adaptive fuzzy controller (AFC) is designed to deal with the problem of input saturation, and the vessel's unmeasured states including unknown dynamic model parameters and time-varying [28]. The development of adaptive fuzzy control has got lots of outstanding results to deal with problems of adapted to the influence of uncertainty and disturbance of nonlinear systems in pieces of literature [2,4,29–31]. Related to fuzzy tuning, a control method is performed for linearized systems [32] with uncertainties using the sliding mode verified by a two-mass system. Moreover, robust adaptive control used a new scheme that estimates the bound of the disturbance by using a sliding surface shown the effectiveness of the proposal [33]. To enhance the robust stability of DPS, H_∞ robust recurrent cerebellar model articulation is investigated in [17] for designing control systems. Thus, most fuzzy algorithms including adaptive which are not applied in the field of guaranteed the performance of robust tracking in path planning control for the vessel.

To overcome the aforementioned problems, we present a novel model of the robust adaptive fuzzy controller (RAFC) to cope with position control for a class of nonlinear vessel's DPS. The contributions of the paper are presented as follows:

- (1) We propose the model of adaptive fuzzy control for vessel's DPS based on soft fuzzy rules, the AFC with the adaptation coefficient δ_{AFC} is constructed to improve the membership function (MF) of the fuzzy controller in order to reduce the error in the vessel's path planning control and to maintain the vessel overshoot and vessel fluctuation in the stability criterion.
- (2) We improve the robustness of the system by suggesting the coefficient δ_{RC} aiming to guarantee the DPS control process, and then the H_∞

performance of robust tracking is proved by the Lyapunov theory. By the way, the robust adaptive coefficient δ_i of the proposed controller keeps the DPS satisfying both quality and robustness.

- (3) We test a simulation experiment comprising two case studies. The comparing of the proposed RAFC with fuzzy, MFC, AFC confirmed the efficiency of the suggested approach.

The remainder of this paper is organized as follows. In Section 2, we introduce preliminaries and problem statements of the nonlinear motion of the support vessel with assumptions and a remark. The proposed robust adaptive fuzzy control model is presented in Section 3. Next section, we dedicated numerical case studies to show the simulation results, analysis and evaluation of the proposed RAFC model. Finally, we conclude the paper in Section 4.

2. Preliminaries and problem statement

2.1. Modelling of vessel dynamic positioning

The vessel model system in DPS mode (described in Figure 1) consists of two separate coordinate systems [34] established as below: the first coordinate system is a vessel fixed non-inertial frame $O - XYZ$ and the second coordinate is the inertial system approximated to the earth frame $O_0 - X_0Y_0Z_0$. The DPS with three degrees of freedom, namely, surge, sway and yaw expressed as

$$\dot{\eta} = J(\psi)v \quad (1)$$

$$M\dot{v} + Dv = \tau - \tau_{en}(\eta, v, t) \quad (2)$$

Let a vector $\eta = (x, y, \psi)^T$ describes the position (x, y) and heading (ψ) of the absolute coordinate system $X_0Y_0Z_0$. The vector $v = (u, v, r)^T$ expresses the vector consisting of the vessel velocities in the direction of translation – surge, drift – sway and rotation – yaw. $M \in R^{3 \times 3}$ and $D \in R^{3 \times 3}$ describe the inertia matrix and damping matrix for the vessel motion [35], respectively. The transformation matrix $J(\psi) \in R^{3 \times 3}$ is expressed as

$$J(\psi) = \begin{bmatrix} \cos(\psi) & -\sin(\psi) & 0 \\ \sin(\psi) & \cos(\psi) & 0 \\ 0 & 0 & 1 \end{bmatrix} \quad (3)$$

The thruster and propeller systems create the force τ which controls the vessel motion. Vector $\tau_{en}(\eta, v, t)$ signifies the environmental forces.

Considering the actual thruster situation with τ_{\max} and τ_{\min} are the physical limitations, respectively represent the maximum and minimum control forces or moments, the control forces and moment [36] are described as

$$\tau = \begin{cases} \tau_{\max}, & \text{if } \tau \geq \tau_{\max} \\ \tau, & \text{if } \tau_{\min} < \tau < \tau_{\max} \\ \tau_{\min}, & \text{if } \tau \leq \tau_{\min} \end{cases} \quad (4)$$

Lemma 1 [37]: For the continuous function $\tau_{eni}(\eta, v, t): \mathfrak{R}^3 \times \mathfrak{R}^3 \times \mathfrak{R} \rightarrow \mathfrak{R} (i = 1, 2, 3)$, there exist positive, smooth and nondecreasing functions $p_i(\eta, v): \mathfrak{R}^3 \times \mathfrak{R}^3 \rightarrow \mathfrak{R}^+$ and $w_i(t): \mathfrak{R} \rightarrow \mathfrak{R}^+$ such that

$$|\tau_{eni}(\eta, v, t)| \leq p_i(\eta, v) + w_i(t), (i = 1, 2, 3) \quad (5)$$

Lemma 1 allows to separate the multivariable environmental disturbance term $\tau_{eni}(\eta, v, t)$, for $i = 1, 2, 3$, into a bounding function in terms of v, η , the vessel internal states, and a bounding function in terms of t , which generally includes uncertainties and external impacts.

Assumption 1: M and D are certainty matrices; $\tau_{en}(t)$ is unknown time-varying but bounded while $w_i(t)$ is the time-dependent function and satisfies $w_i(t) \leq \omega_m$, where ω_m is an uncertain positive constant.

Assumption 2: Environmental forces (τ_{en}) is the main factor acting on the hull during the vessel's control, τ_{en} are positively bounded.

Remark 1: Note that the purpose of the control solutions is to maintain the vessel's heading along the route. When the ship is operating, τ_{en} is unknown and it varies with an extremely high value over time, causing the control states to be over large in amplitude, leading to failure of control, loss of direction and deviation of the vessel gradually out of the path planning.

We aim to develop the RAFC strategy for the DPS under the problem of *Assumptions 1 and 2*. The performances are held on the expected values of the vessel position and heading, while the robust law guarantees the control signal in the bounded robustness. Therefore, enhancing the performance of the vessel control assists the DPS fast-forward to a stable domain.

2.2. Stages and goal of the RAFC

The traditional fuzzy controller always maintains a certain level of interaction. In the actual conditions, the uncertainties and tremendous impacts make the vessel's position to be erroneous. Thus, the vessel's path trajectory will be out of following the set-point as the conditions outlined in *Assumptions 1 and 2*. The idea tries to overcome the aforementioned actual conditions, the study suggests a novel AFC in which the MFs are adjusted by adaptive coefficient δ_{AFC} .

Besides that, the environmental force (τ_{en}) is considered to be the main force causing error and uncertainty in the DPS control process. Therefore, the uncertainties of the mentioned system can not fully be solved if we selected the AFC for the vessel trajectory control. From that statement, the purpose of our strategy is to merge the robust controller δ_{RC} in synchronous with the AFC structure using the adaptation law by regulating coefficient δ_{AFC} . Let the robust adaptive coefficient

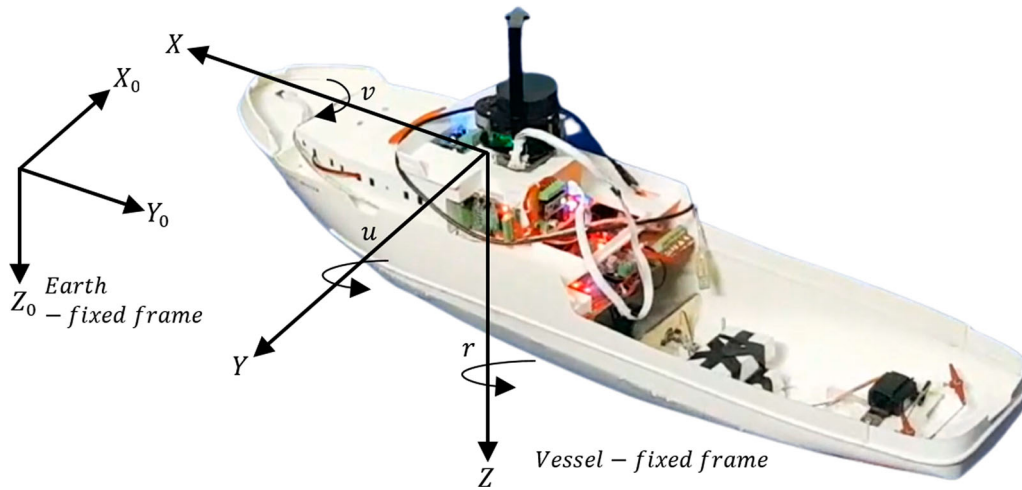


Figure 1. Definition of the earth-fixed and the vessel fixed reference frames.

δ_i be

$$\delta_i = \delta_{AFC} - \delta_{RC} \quad (6)$$

Because of this, these requirements are considered into account in the proposed strategy design is to develop the robust adaptive coefficient δ_i such that the vessel motion is reached with guaranteed robustness bounded. However, the robust coefficient δ_{RC} obeys the δ_i calibration values uniformly ultimately limited. Hence, the mechanism of the proposed model is expressed by Figure 2 consists of two main stages as follows:

- The first stage: Find out the adaptation coefficient δ_{AFC} of the AFC controller to maintain the vessel overshoot and vessel fluctuation in the stability criterion.
- The second stage: Suggest the coefficient δ_{RC} aiming to guarantee the DPS control process in the robust bounded.

With the goal mentioned above, the RAFC strategy intends to define the calibration coefficient δ_i . Thus, the system not only meets the high control quality but also maintains stability robustness. The operation mechanism of adaptive calibration and robust calibration for δ_i coefficient present in the next section.

3. Robust adaptive fuzzy control strategy

We present a fuzzy model including the input variables e , de/dt and output variable τ in this section [38]. This model is composed of a collection of rules and rule consequences, which are frequently assumed to be linear functions of the inputs [39]. The group of If-Then rules is written in the rule notation form within θ^i as

$$R_i : \text{If } \hat{z}_1 \text{ is } L_1^i \dots \text{ and } \hat{z}_n \text{ is } L_n^i \text{ then } \tau \text{ is } \theta^i \quad (7)$$

for $\theta^i \in R^h$ and $L_1^i, L_2^i, \dots, L_n^i \in R^h$ are the fuzzy sets of output variables and input variables [40]. Using the

Max-Prod inference rule, the singleton fuzzifier and the centre averaged defuzzifier, the output variable τ is computed as

$$\tau(\hat{z}) = \frac{\sum_{i=1}^h \theta^i \left[\prod_{j=1}^n \mu_{L_j^i}(\hat{z}_j) \right]}{\sum_{i=1}^h \left[\prod_{j=1}^n \mu_{L_j^i}(\hat{z}_j) \right]} \quad (8)$$

where h indicates the number of if-then rules, $\mu_{L_j^i}(\hat{z}_j)$ represents the MFs. Notate

$$\varphi(\hat{z}) = [\varphi^1, \varphi^2, \dots, \varphi^h]^T \in R^h \quad (9)$$

as the fuzzy basis functions with φ is determine as follows:

$$\varphi(\hat{z}) = \frac{\left[\prod_{j=1}^n \mu_{L_j^i}(\hat{z}_j) \right]}{\sum_{i=1}^h \left[\prod_{j=1}^n \mu_{L_j^i}(\hat{z}_j) \right]} \quad (10)$$

In the AFC model, the MFs variable is dynamically corrected with the δ_i^T adjustable vector corresponding to θ^i ($i = 1, 2, \dots, h$). From there, the output variable τ (8) can be presented as the linearization parametric form

$$\tau(\hat{z}) = \delta_i^T \varphi(\hat{z}) = f(\hat{z}|\delta_i) \quad (11)$$

Lemma 2 [41]: Let $f(\hat{z})$ be a continuous function defined on a compact set Ω . Then, for any constant $\varepsilon > 0$, there exists a fuzzy system (10) in the form of Equation (11) such that

$$\sup_{\hat{z} \in \Omega} |f(\hat{z}) - f(\hat{z}|\delta_i)| < \varepsilon \quad (12)$$

In the working condition, D , M are assumed to be deterministic under *Assumption 1*, but control forces τ of the DPS cannot define exactly under the environment impact τ_{en} . Because of this, we develop the AFC controller for reducing the disturbances affecting the stability of the system [17]. Let suppose that the optimal parameters of ideal approximation calibration δ_{AFC}^0

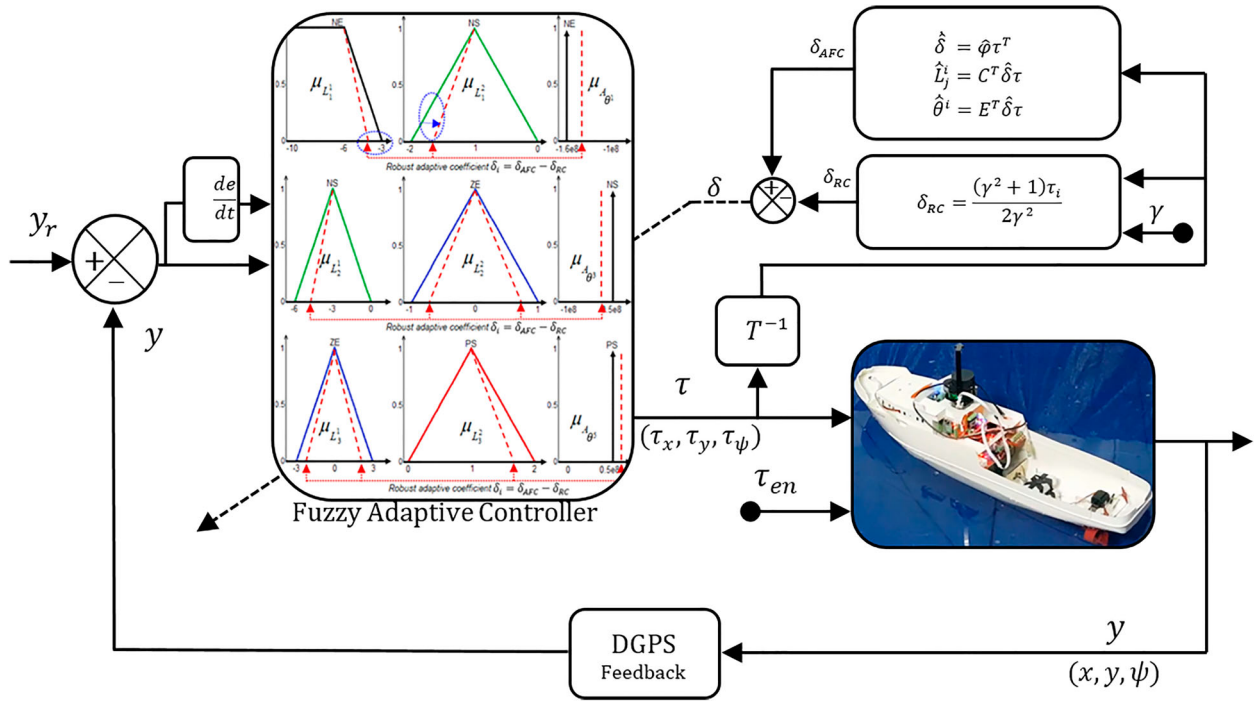


Figure 2. The robust adaptive fuzzy controller structure for DPS.

is performed as

$$\delta_{AFC}^0(L_j^{i0}, \theta^{i0}, \varphi^0) = \delta^{0T} \varphi^0(\hat{z}) \quad (13)$$

where the optimal values of L^i , θ^i , φ are represented by L_j^{i0} , θ^{i0} , φ^0 , respectively. However, the DPS controller cannot meet the optimal goal in the actual condition. Therefore, the estimated parameters δ_{AFC} are used for designing DPS controller as

$$\delta_{AFC}(\hat{L}_j^i, \hat{\theta}^i, \hat{\varphi}) + \delta_{RC} = \hat{\delta}^T \hat{\varphi}(\hat{z}) + \delta_{RC} \quad (14)$$

therein, \hat{L}_j^i , $\hat{\theta}^i$, $\hat{\varphi}$ indicate the estimation values L_j^{i0} , θ^{i0} , φ^0 , respectively. Define the approximation error of DPS controller $\tilde{\delta}$ as

$$\begin{aligned} \tilde{\delta} &= (\delta_{AFC}^0 - \delta_{AFC}) \\ &= (\delta^{0T} \varphi^0(\hat{z}) - \hat{\delta}^T \hat{\varphi}(\hat{z}) - \delta_{RC}) \\ &= (\tilde{\delta}^T \varphi^0(\hat{z}) + \hat{\delta}^T \tilde{\varphi}(\hat{z}) - \delta_{RC}) \end{aligned} \quad (15)$$

for $\tilde{\delta} = \delta^0 - \hat{\delta}$, $\tilde{\varphi} = \varphi^0 - \hat{\varphi}$ is an approximation error between the estimated values and the optimal values.

Theorem 1: For the vessel's DPS with three degrees of freedom (1), (2) and the fuzzy linearization parametric controller is designed as Equation (11), in the operating conditions as *Assumption 1* within *Lemma 2*, the adaptive laws are selected as

$$\hat{\delta} = \hat{\varphi} \tau^T \quad (16)$$

$$\hat{L}_j^i = C^T \hat{\delta} \tau \quad (17)$$

$$\hat{\theta}^i = E^T \hat{\delta} \tau \quad (18)$$

and the approximation error $\tilde{\delta}$ is the smallest satisfy

$$\lim_{t \rightarrow \infty} \|\tilde{\delta}\| = \lim_{t \rightarrow \infty} \|\delta_{AFC}^0 - \delta_{AFC}\| = 0 \quad (19)$$

Then, the path tracking position error will be uniformly ultimately bounded, the system is asymptotically stable.

Proof: This study uses the Taylor series expansion to convert a multi-dimensional receptive-field space into a partly linear form. In two variables, L_j^i and θ^i , linear approximation terms of $\tilde{\varphi}$ gives

$$\begin{aligned} \tilde{\varphi} &= \begin{bmatrix} \tilde{\varphi}_1 \\ \vdots \\ \tilde{\varphi}_k \\ \vdots \\ \tilde{\varphi}_{nb} \end{bmatrix} \\ &= \begin{bmatrix} \left(\frac{\partial \varphi_1}{\partial L_j^i} \right)^T \\ \vdots \\ \left(\frac{\partial \varphi_k}{\partial L_j^i} \right)^T \\ \vdots \\ \left(\frac{\partial \varphi_{nb}}{\partial L_j^i} \right)^T \end{bmatrix} (L_j^{i0} - \hat{L}_j^i)_{|L_j^i = \hat{L}_j^i} \end{aligned}$$

$$+ \begin{bmatrix} \left(\frac{\partial \varphi_1}{\partial \theta^i}\right)^T \\ \vdots \\ \left(\frac{\partial \varphi_k}{\partial \theta^i}\right)^T \\ \vdots \\ \left(\frac{\partial \varphi_{nb}}{\partial \theta^i}\right)^T \end{bmatrix} (\theta^{i0} - \hat{\theta}^i)_{|\theta^i = \hat{\theta}^i} + H_h \quad (20)$$

The estimation of the fuzzy basis function is represented by

$$\varphi^0 = \tilde{\varphi} + C^T \tilde{L}_j^i + E^T \tilde{\theta}^i + H_h \quad (21)$$

Defining and applying

$$\tilde{L}_j^i = L_j^{i0} - \hat{L}_j^i, \tilde{\theta}^i = \theta^{i0} - \hat{\theta}^i \quad (22)$$

and H_h is the higher-order form of Taylor series expansion. Let's take the derivative on both sides of Equation (11) and substitute $\tilde{\varphi} = C^T \tilde{L}_j^i + E^T \tilde{\theta}^i + H_h$ and $\varphi^0 = \hat{\varphi} + \tilde{\varphi}$ into Equation (15), yields

$$\begin{aligned} \dot{\tau}(\hat{z}) &= \tilde{\delta} = (\delta_{AFC}^0 - \delta_{AFC}) \\ &= \tilde{\delta}^T (\hat{\varphi} + C^T \tilde{L}_j^i + E^T \tilde{\theta}^i + H_h) \\ &\quad + \hat{\delta}^T (C^T \tilde{L}_j^i + E^T \tilde{\theta}^i + H_h) - \delta_{RC} \\ &= \tilde{\delta}^T \hat{\varphi} + \hat{\delta}^T (C^T \tilde{L}_j^i + E^T \tilde{\theta}^i) + \tilde{\delta}^T (C^T \tilde{L}_j^i + E^T \tilde{\theta}^i) \\ &\quad + \delta^{0T} H_h - \delta_{RC} \\ &= \tilde{\delta}^T \hat{\varphi} + \hat{\delta}^T (C^T \tilde{L}_j^i + E^T \tilde{\theta}^i) - \delta_{RC} + U_r \end{aligned} \quad (23)$$

Notate

$$U_r = \tilde{\delta}^T (C^T \tilde{L}_j^i + E^T \tilde{\theta}^i) + \delta^{0T} H_h \quad (24)$$

as the annotation of the uncertainties and environmental effects. Consider the Lyapunov function candidate for the whole DPS as [42]

$$V(\tau, \tilde{\delta}, \tilde{L}_j^i, \tilde{\theta}^i) = \frac{1}{2} \tau^T \tau + \frac{1}{2} \tilde{\delta}^T \tilde{\delta} + \frac{1}{2} \tilde{L}_j^{iT} \tilde{L}_j^i + \frac{1}{2} \tilde{\theta}_j^{iT} \tilde{\theta}_j^i \quad (25)$$

Derivative two sides of the Equation (25), we have

$$\begin{aligned} \dot{V}(\tau, \tilde{\delta}, \tilde{L}_j^i, \tilde{\theta}^i) &= \tau^T \dot{\tau} + \tilde{L}_j^{iT} \dot{\tilde{L}}_j^i + \tilde{\theta}^{iT} \dot{\tilde{\theta}}^i + \tilde{\varphi}^T \dot{\tilde{\varphi}} \\ &= \tau^T (\tilde{\delta}^T \hat{\varphi} + \hat{\delta}^T (C^T \tilde{L}_j^i + E^T \tilde{\theta}^i) \\ &\quad - \delta_{RC} + U_r) - \tilde{\delta}^T \dot{\tilde{\delta}} - \tilde{L}_j^{iT} \dot{\tilde{L}}_j^i - \tilde{\theta}^{iT} \dot{\tilde{\theta}}^i \end{aligned} \quad (26)$$

Applying $\tau^T \dot{\tilde{\delta}}^T \hat{\varphi} = \tilde{\delta}^T \hat{\varphi} \tau^T$, so the Equation (26) is reproduced by

$$\begin{aligned} \dot{V}(\tau, \tilde{\delta}, \tilde{L}_j^i, \tilde{\theta}^i) &= \tilde{\delta}^T (\hat{\varphi} \tau^T - \dot{\hat{\varphi}}) + \tilde{L}_j^{iT} (C^T \hat{\delta} \tau - \dot{\hat{L}}_j^i) \\ &\quad + \tilde{\theta}^{iT} (E^T \hat{\delta} \tau - \dot{\hat{\theta}}^i) + \tau^T U_r - \tau^T \delta_{RC} \end{aligned} \quad (27)$$

Using the adaptive laws equations (defined by Equations (16)–(18)) and the approximation error (19), Equation (27) can be performed as

$$\dot{V}(\tau, \tilde{\delta}, \tilde{L}_j^i, \tilde{\theta}^i) = -\tau^T \|\delta_{RC} - U_r\| \leq 0 \quad (28)$$

By using the Lyapunov function candidate, $\dot{V} \leq 0$ is uniformly continuous and τ approaches to 0. From there, the path tracking position error \tilde{L}_j^i , $\tilde{\theta}^i$ and $\tilde{\varphi}$ are bounded. We get

$$\lim_{t \rightarrow \infty} (-\tau^T \|\delta_{RC} - U_r\|) = \lim_{t \rightarrow \infty} \dot{V}(\tau, \tilde{\delta}, \tilde{L}_j^i, \tilde{\theta}^i) = 0 \quad (29)$$

Hence, the approximation error $\tilde{\delta} \rightarrow 0$ as $t \rightarrow \infty$, the system is asymptotically stable, then *Theorem 1* is proven.

The adaptive laws of the AFC controller are suggested in *Theorem 1* to decrease the errors during the DPS control process. The goal of the adjustment coefficient δ_{RC} is to remove the uncertainties that the AFC structure does not handle well. Let derivative of Equation (27), we get

$$\dot{V}(\tau, \tilde{\delta}, \tilde{L}_j^i, \tilde{\theta}^i) \leq \tau^T U_r - \tau^T \delta_{RC} = \sum_{i=1}^n (\tau_i U_{ri} - \tau_i \delta_{RC}) \quad (30)$$

Let the desired robust controller be

$$\delta_{RC} = \frac{(\gamma^2 + 1)\tau_i}{2\gamma^2} \quad (31)$$

where γ_i are the specified uncertainties reduction.

Theorem 2: By virtue of *Assumption 1* and *Theorem 1*, to joint AFC controller (11) with the robust controller (31), the RAFC achieves the asymptotic stabilization by suitably choosing the H_∞ performance of robust path tracking as

$$\sup_{U_{ri} \in L_2[0, T]} \sum_{i=1}^n \left(\frac{\tau_i}{U_{ri}} \leq \gamma_i \right) \quad (32)$$

Notate

$$\left| |\tau_i|^2 = \int_{t=0}^T \tau_i^2 dt, \left| |U_{ri}|^2 = \int_{t=0}^T U_{ri}^2 dt \right. \right. \quad (33)$$

Proof: By replacing (31) into (30), Equation (30) can be rewritten as

$$\begin{aligned} \dot{V}(\tau, \tilde{\delta}, \tilde{L}_j^i, \tilde{\theta}^i) &\leq \sum_{i=1}^n \left(\tau_i U_{ri} - \tau_i \frac{(\gamma_i^2 + 1)\tau_i}{2\gamma_i^2} \right) \\ &\leq \sum_{i=1}^n \left(\tau_i U_{ri} - \frac{1}{2} \tau_i^2 - \frac{1}{2\gamma_i^2} \tau_i^2 \right) \\ &\leq \sum_{i=1}^n \left(-\frac{1}{2} \tau_i^2 - \frac{1}{2} \left(\frac{\tau_i}{\gamma_i} - \gamma_i U_{ri} \right)^2 + \frac{\gamma_i^2 U_{ri}^2}{2} \right) \end{aligned}$$

$$\leq \sum_{i=1}^n \left(-\frac{1}{2} \tau_i^2 + \frac{\gamma_i^2 U_{ri}^2}{2} \right) \quad (34)$$

Integrating (34) on both sides with respect $t = 0$ to $t = \infty$, we get

$$V(T) - V(0) \leq \sum_{i=1}^n \left(-\frac{1}{2} \int_{t=0}^{\infty} \tau_i^2 dt + \frac{\gamma_i^2}{2} \int_{t=0}^{\infty} U_{ri}^2 dt \right) \quad (35)$$

By using the value of the Lyapunov function, $V(t) \geq 0$, so the inequality in Equation (35) is performed as follows:

$$\sum_{i=1}^n \frac{1}{2} \int_{t=0}^T \tau_i^2 dt \leq V(0) + \sum_{i=1}^n \frac{\gamma_i^2}{2} \int_{t=0}^T U_{ri}^2 dt \quad (36)$$

Based on the candidate Lyapunov in Equation (25), the inequalities of Equation (36) is represented as

$$\begin{aligned} \sum_{i=1}^n \frac{1}{2} \int_{t=0}^T \tau_i^2 dt &= \tau^T(0) \tau(0) \\ &+ \frac{1}{2} \tilde{L}_j^{iT}(0) \tilde{L}_j^i(0) + \frac{1}{2} \tilde{\theta}^{iT}(0) \tilde{\theta}^i(0) \\ &+ \frac{1}{2} \tilde{\varphi}^T(0) \tilde{\varphi}(0) + \sum_{i=1}^n \frac{\gamma_i^2}{2} \int_{t=0}^T U_{ri}^2 dt \end{aligned} \quad (37)$$

The initial conditions are $\tau = 0$, $\tilde{L}_j^i = 0$, $\tilde{\theta}^i = 0$ and $\tilde{\varphi} = 0$ for the DPS control process. We have

$$\sum_{i=1}^n \frac{1}{2} \int_{t=0}^T \tau_i^2 dt = \sum_{i=1}^n \frac{\gamma_i^2}{2} \int_{t=0}^T U_{ri}^2 dt \quad (38)$$

Applying the approximation error $\tilde{\delta}$ (*Theorem 1*) for (38), it is concluded that

$$\lim_{t \rightarrow 0} \|U_{ri}\|^2 = 0 \quad (39)$$

As the result, Equation (39) indicates that the H_∞ performance of robust path tracking (32) tends to infinity and guarantees the DPS control variables in the robustness bounded. *Theorem 2* has been proved.

4. Simulation and evaluation studies

4.1. Numerical simulations

The effectiveness evaluations between the proposed RAFC and the AFC [3] are performed on the Northern Clipper support vessel [22] by simulation. The main parameters of the vessel are the breadth of 18 m, design mass 4.5915×10^6 kg, the overall length of 82 m, and draught 4.6 m. Structural parameters of the vessel are

performed by

$$D = \begin{bmatrix} 5.0242 \times 10^4 & 0 & 0 \\ 0 & 2.7229 \times 10^5 & -4.3933 \times 10^6 \\ 0 & -4.3933 \times 10^6 & 4.1894 \times 10^8 \end{bmatrix}$$

$$M = \begin{bmatrix} 5.3122 \times 10^6 & 0 & 0 \\ 0 & 8.2831 \times 10^6 & 0 \\ 0 & 0 & 3.7454 \times 10^9 \end{bmatrix}$$

In this paper, the simulation is performed by the Matlab 2016a application, and the results are shown in Figures 3 and 4. The simulation result of the RAFC controller (blue line) is evaluated in comparison with the AFC controller (red line). However, an actual path of the vessel (x, y) and heading (ψ) are maintained at the desired value expressed by Figures 3(a,b) and 4(a,b). Figures 3(c) and 4(c) indicate that the RAFC controller and AFC controller can control the vessel's motion to steer at the desired path in both two cases. Moreover, in the vessel's path approach, the environmental forces make the performance of the DPS control cannot be guaranteed at a required level. On the other hand, the environment forces [43] are caused by the wave force, wind force and current force, named τ_{en} , which is expressed as

$$\tau_{en} = \tau_{wa} + \tau_{wi} + \tau_{cur} \quad (40)$$

The forces of wave, wind and currents are registered as the most three environmental forces that affect the path planning of the vessel. The detailed environmental forces are introduced in the next subsection.

4.2. Environment parameters

The wave force is described as follow:

$$\begin{aligned} \tau_{wa} &= \zeta_{qr}(x, y, t) \\ &= \zeta_{aqr} \sin(\omega_q t + \phi_{qr} - k_q(x \cos \psi_r + y \sin \psi_r)) \end{aligned} \quad (41)$$

therein, ζ_{qr} represents the wave amplitude. ω_q expresses the wave spectrum peak frequency and the dispersion relation $\omega_q = \sqrt{kg}$ with g notate the acceleration of gravity. The amplitude of wave phase angle ϕ_{qr} is selected between 0 and 2π . The number of waves is $k_q = 2\pi/\lambda_q$, where λ_q defines the wavelength with wave direction limit $\psi_r = 0$. The wind speed V_w and wind direction β_w are modelled as the slowly varying quantities. The wind forces $\tau_{wi} = [X_{wi}, Y_{wi}]^T$ are defined as

$$\begin{aligned} X_{wi} &= 0.5 D_X g_R \rho_w V_R^2 C_T \\ Y_{wi} &= 0.5 D_Y g_R \rho_w V_R^2 C_T \end{aligned} \quad (42)$$

where D_X and D_Y represent the traction of wind acting on the place of ichnography C_T . Besides, V_R stands for

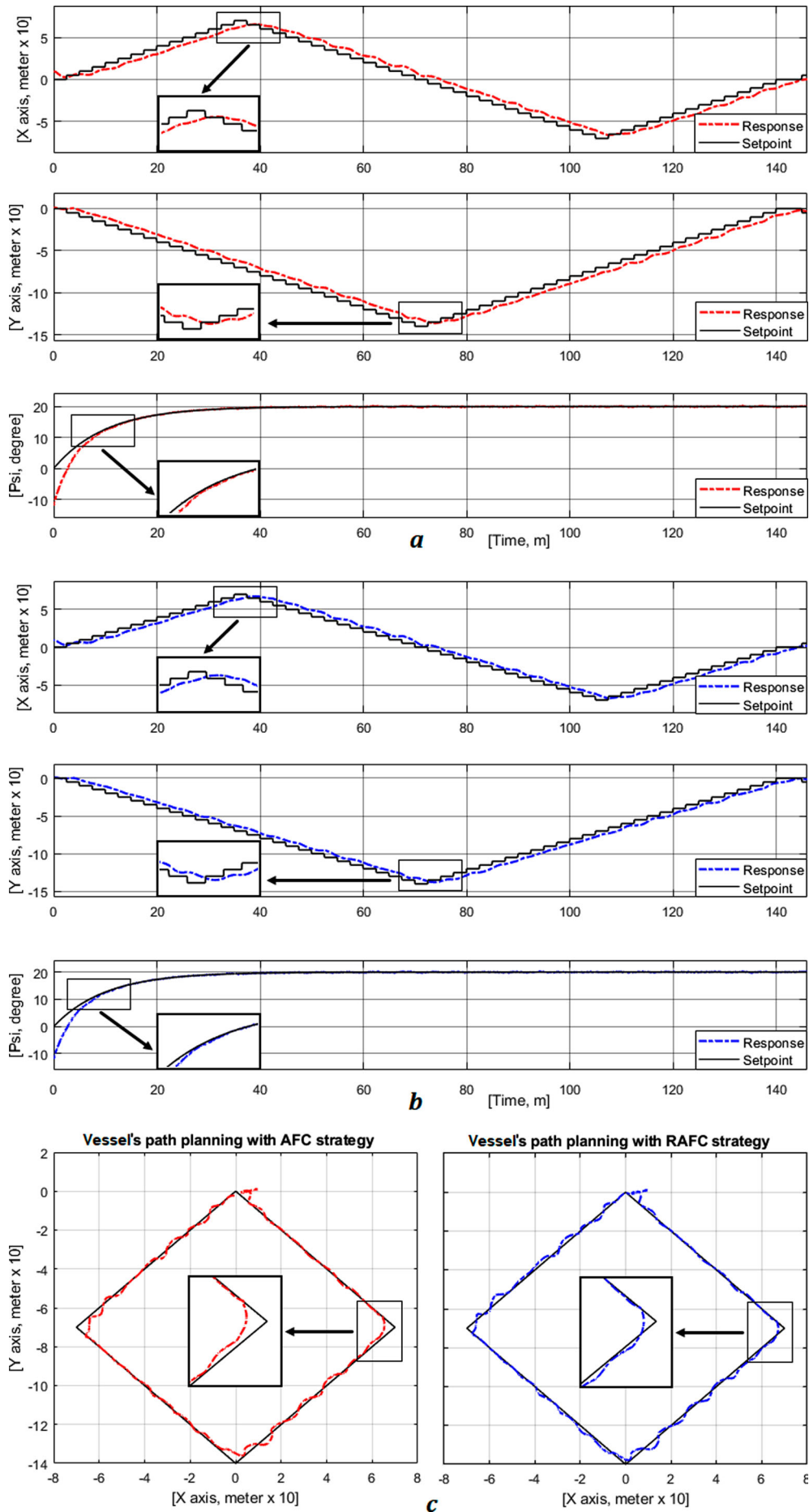


Figure 3. The simulation results consist two controllers in the case study 1. (a) Actual position (x, y) and the vessel heading ψ using the AFC controller. (b) Actual position (x, y) and the vessel heading ψ using the RAFC controller. (c) Trajectory of the vessel's path in xy -plane

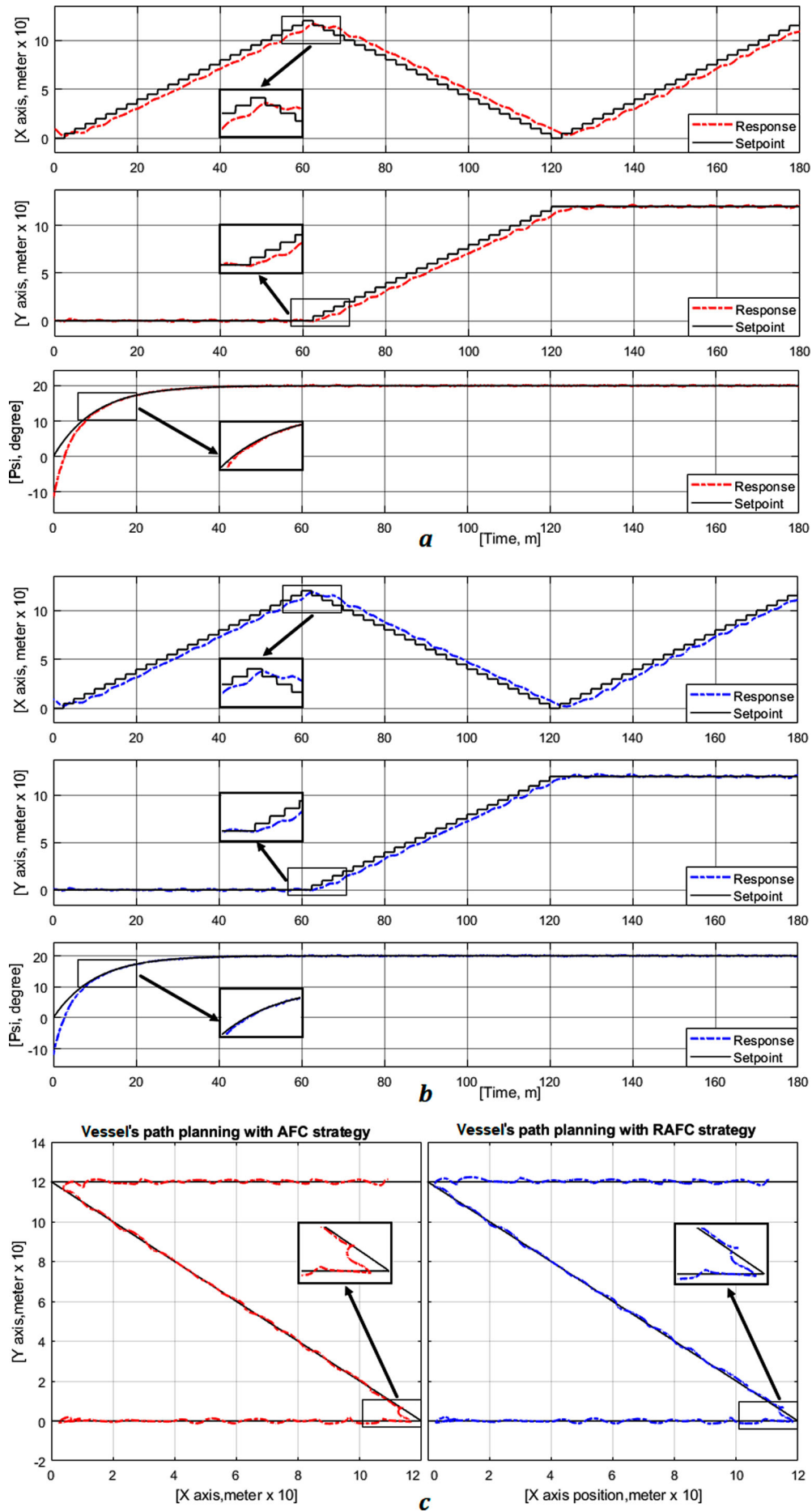


Figure 4. The simulation results consist two controllers in the case study 2. (a) Actual position (x, y) and the vessel heading ψ using the AFC controller. (b) Actual position (x, y) and the vessel heading ψ using the RAFC controller. (c) Trajectory of the vessel's path in xy -plane

wind speed and g_R is the wind direction affecting vessel motion. The wind simulation parameters are sorted as follows: $A_L = 2.4$, $A_T = 9.34$, wind speed $V_\omega = 2$ m/s and the angle of impact wind $\beta_\omega = 20^\circ$.

$$\begin{aligned} V_R &= V_w \\ g_R &= \beta_w - \psi_L - \psi_H \end{aligned} \quad (43)$$

The simulation parameters for current factor are set to their default values accepted as follows: $V_C = 2$ m/s, vessel direction $\beta_C = 30^\circ$, low frequency and high frequency of rotation are ignored $\psi_L = \psi_H = 0$.

$$\begin{aligned} \tau_{cur} &= [u_c, v_c, 0]^T \\ u_c &= V_c \cos(\beta_c - \psi_L - \psi_H) \\ v_c &= V_c \sin(\beta_c - \psi_L - \psi_H) \end{aligned} \quad (44)$$

Besides that, the operation state of the propeller is subject to turbulence flows, which is also a cause of structural uncertainty in the vessel dynamics. The viscous damping force due to turbulence flows can be modelled as

$$f(u) = -\frac{1}{2} \rho C_D(R_e) A |u| u \quad (45)$$

therein A shows the projected cross-sectional area underwater, and u presents the vessel velocity based on the water density ρ . $C_D(R_e)$ is the drag coefficient with the Reynolds number as follow:

$$R_e = \frac{uL}{\nu} \quad (46)$$

where ν expresses the coefficient of kinematic viscosity and L represents the body length of the vessel. The DPS will only operate under certain allowable working conditions of weather, equivalent to the force of turbulence flows being small and limited. Therefore, this study does not consider the effect of the viscous damping force and the Reynolds number.

4.3. Case study 1

In case study 1, the response comparisons between the proposed controller (RAFC) and the other controller (AFC) are realized to evaluate the effectiveness of the proposed controller under environmental conditions (expressed at Table 2). The RAFC controller with the stable goal (expressed at Equation (32)) is carried out on the Northern Clipper model for keeping the desired trajectory of the vessel's path (presented by Table 3) in around 140 min from the reference value $[0, 0 \text{ m}, 0^\circ]$. The performances of the RAFC strategy and AFC strategy are shown in Figure 3. In which the limitations of robust adaptive coefficients $\delta_{min} \leq \delta_i \leq \delta_{max}$ and the limitations of actual thruster $\tau_{min} \leq \tau \leq \tau_{max}$ are established as

$$\delta_{min}(\delta_x = -9.3435e^6, \delta_y = -8.4121e^6,$$

Table 2. Environmental parameters for simulation.

Description	Symbol	Dimension
Wave height	H_s	0.8 m
Wave spectrum peak frequency	ω_0	0 rad/s
Wave direction	ψ_0	30°
Spreading factor	s	2
Number of frequencies	N	20
Number of directions	M	10
Cutoff frequency factor	ζ	3
Wave component energy limit	k	0.005
Wave direction limit	ψ_{lim}	0
Wind traction	A_T	2.4
Wind speed	V_ω	2 m/s
Angle of impact wind	β_ω	20°
Current speed	V_c	2 m/s
Vessel direction	β_c	30°
Low and high frequency of rotation	ψ_L, ψ_H	0°
Dominating wave frequency	w_0	0.8976 rad/s
Damping coefficient	λ	0.1
Wave intensity	σ	$\sqrt{2}$

$$\delta_\psi = -1.5025e^7);$$

$$\delta_{max}(\delta_x = 9.3435e^6, \delta_y = 8.4121e^6, \delta_\psi = 1.5025e^7);$$

$$\tau_{min}(\tau_x = -2.268 \times 10^6 \text{ kN}, \tau_y = -2.272 \times 10^6 \text{ kN},$$

$$\tau_\psi = -3.674 \times 10^6 \text{ kN});$$

$$\tau_{max}(\tau_x = 2.268 \times 10^6 \text{ kN}, \tau_y = 2.272 \times 10^6 \text{ kN},$$

$$\tau_\psi = 3.674 \times 10^6 \text{ kN}).$$

The simulation results are pointed in Figure 3. These results indicate the RAFC controller can satisfy the engineering needs. The vessel's path tracking of RAFC controller is expressed in Figure 3(c), from which it can be seen that the calibration coefficient $\delta_i(\delta_x, \delta_y, \delta_\psi)$ is guaranteed in robustness bounded. Further, the vessel trajectories are shown in Figure 3(a,b) meet the requirements of the fluctuation and overshoot aspect in comparison with the AFC controller. Besides this, the comparisons between the proposed controller concept and the other concept as fuzzy [39], multi-cascade fuzzy (MCF) [34] and AFC [3] are carried out and synthesized in Table 4. In the detail, the fluctuation amplitude of the proposed RAFC is lower than those of the fuzzy, the MCF and the AFC approximately 0.07, 0.05 and 0.04 m, respectively. In the overshoot aspect, the amplitude of the fuzzy, the MCF, the AFC and the RAFC are 0.31, 0.27, 0.25 and 0.22 m, respectively. However, the RAFC strategy can achieve the absolute smallest fluctuation and overshoot which defines the DPS control process operates better than the others. Meanwhile, the response time of the RAFC is slightly slower indicated that the robust adaptive fuzzy control strategy takes more time consuming than normal concepts such as the MCF and the AFC.

4.4. Case study 2

In this subsection, changing the vessel's path simulations are performed to prove the robustness and adaptability of the RAFC strategy under the impacts

Table 3. The desired trajectory of the vessel's path in case study 1.

Time [m]	x, y, ψ [m, m, d]	Time [m]	x, y, ψ [m, m, d]	Time [m]	x, y, ψ [m, m, d]	Time [m]	x, y, ψ [m, m, d]
05	10,-10,20	40	60,-80,20	75	-10,-130,20	110	-60,-60,20
10	20,-20,20	45	50,-90,20	80	-20,-120,20	115	-50,-50,20
15	30,-30,20	50	40,-100,20	85	-30,-110,20	120	-40,-40,20
20	40,-40,20	55	30,-110,20	90	-40,-100,20	125	-30,-30,20
25	50,-50,20	60	20,-120,20	95	-50,-90,20	130	-20,-20,20
30	60,-60,20	65	10,-130,20	100	-60,-80,20	135	-10,-10,20
35	70,-70,20	70	00,-140,20	105	-70,-70,20	140	00,00,20

Table 4. A response comparison of different controllers for case study 1.

Aspect	Fuzzy[39]	MCF[34]	AFC[3]	Proposed RAFC
Membership functions	45	45	45	45
Response time	24 s	22 s	20 s	21 s
Fluctuation	0.28 m	0.26 m	0.25 m	0.21 m
Overshoot	0.31 m	0.27 m	0.25 m	0.22 m

Table 5. The desired trajectory of the vessel's path in case study 2.

Time [m]	x, y, ψ [m, m, d]	Time [m]	x, y, ψ [m, m, d]	Time [m]	x, y, ψ [m, m, d]
00	00,00,00	60	120,00,20	120	00,120,20
05	05,00,20	65	115,05,20	125	05,120,20
10	15,00,20	70	105,15,20	130	15,120,20
15	25,00,20	75	95,25,20	135	25,120,20
20	35,00,20	80	85,35,20	140	35,120,20
25	45,00,20	85	75,45,20	145	45,120,20
30	55,00,20	90	65,55,20	150	55,120,20
35	65,00,20	95	55,65,20	155	65,120,20
40	75,00,20	100	45,75,20	160	75,120,20
45	85,00,20	105	35,85,20	165	85,120,20
50	95,00,20	110	25,95,20	170	95,120,20
55	105,00,20	115	15,105,20	175	105,120,20
60	115,00,20	120	05,115,20	180	115,120,20

of environmental conditions (given by Table 2) and parameter uncertainties. The limitations of robust adaptive coefficients $\delta_{min} \leq \delta_i \leq \delta_{max}$ and the limitations of actual thruster $\tau_{min} \leq \tau \leq \tau_{max}$ are selected as same as case study 1 as below

$$\begin{aligned} \delta_{min}(\delta_x = -9.3435e^6, \delta_y = -8.4121e^6, \\ \delta_\psi = -1.5025e^7); \\ \delta_{max}(\delta_x = 9.3435e^6, \delta_y = 8.4121e^6, \delta_\psi = 1.5025e^7); \\ \tau_{min}(\tau_x = -2.268 \times 10^6 kN, \tau_y = -2.272 \times 10^6 kN, \\ \tau_\psi = -3.674 \times 10^6 kN); \\ \tau_{max}(\tau_x = 2.268 \times 10^6 kN, \tau_y = 2.272 \times 10^6 kN, \\ \tau_\psi = 3.674 \times 10^6 kN). \end{aligned}$$

are applied to control the Northern Clipper support vessel for maintaining the desired trajectory. The desired trajectory of the vessel's path is provided in detail in Table 5.

The comparison performances in Table 6 indicate that the overshoot amplitude is less than the AFC controller 0.02 m. It is worth noting that the fluctuation amplitude of RAFC is smaller than those of the fuzzy,

Table 6. A response comparison of different controllers for case study 2.

Aspect	Fuzzy [39]	MCF [34]	AFC [3]	Proposed RAFC
Membership functions	45	45	45	45
Response time	21 s	19 s	18 s	20 s
Fluctuation	0.26 m	0.25 m	0.23 m	0.21 m
Overshoot	0.27 m	0.24 m	0.22 m	

the MCF and the AFC approximately 0.05, 0.04 and 0.02 m, respectively. However, the proposed controller is restrained in the response time aspect, in which the RAFC strategy in the 20 s compared to the other concepts as MCF, and AFC are 19 and 18 s, respectively. The quality of the DPS control process which consists of the overshoot and fluctuation aspect is significantly enhanced.

The proposed RAFC can meet the technical requirements under the impacts of uncertainties and environmental forces. Moreover, the simulation results, which are represented by Figure 4, are satisfied in the fluctuation aspect. The RAFC controller can satisfy the smallest overshoot, and verify the position response better than the AFC controller. Nevertheless, the minimum response time of the RAFC is insignificantly better. The last but not less, the proposed RAFC approach reaches the terms of *Assumption 1*, *Assumption 2* and *Remark 1*. Generally, the portable control gains δ_{AFC} of the AFC controller have the adaptability to environmental influences but has not had the robustness to oppose the uncertainties, and this weakness is overcome by the proposed robust solution, resulting in the system reaches control quality, performance and stability. Two case studies have proven the correctness of the proposed controller. Nevertheless, experimental studies are also needed to increase the confirmation of this solution.

4.5. Summarizing simulation results

In this section, the authors provide two case studies in the simulation section of the paper to show their significance (replace experiment). First, multiple coordinate points are used to build motion trajectories of the vessel (as illustrated in Table 3). In reality, the authors performed several trials using algorithms of fuzzy [39], MCF [34], AFC [3], as well as the suggested RAFC,

to compare results. Then, the two primary characteristics of DPS fluctuation and overshoot are compared in Table 5 with RAFC being the least in this group. However, there isn't much analysis in the simulation in terms of robustness according to Theorem 1 and proof employing the Lyapunov criterion. Nevertheless, to compare the efficiency, only the results of two solutions are shown, AFC and RAFC. Specifically, in case study 1, the authors present the results of DPS control in ideal weather conditions, two methods show quite similar results. Whereas in case 2, using the zigzag trajectory (Table 5) and eventually the vessel affected by weather and uncertainty, the result shows that the proposed RAFC gives a better response (Figure 4). Finally, the proposed method demonstrates good stability and robustness over existing algorithms by mathematical demonstration and practical simulation with various vessel path tracking scenarios and conditions.

5. Conclusion

The control model of DPS plays an important role in improving the efficiency of the vessel in most working conditions. In this paper, the proposed RAFC designs for the DPS control process under the influences of environment and uncertainties. The novel approach is competent in adapting itself to certain and uncertain impacts while guaranteeing the robustness of the DPS operation, proof by handling Lyapunov theory. The simulation experimental of two case studies has verified the effectiveness of the proposed strategy compared with the other. More specifically, the RAFC controller calibrates coefficient $\delta_i(\delta_x, \delta_y, \delta_\psi)$ which is guaranteed in robustness bounded to help the vessel keep the path tracking while other algorithms such as MCF and AFC have not mentioned or achieved. However, further experimental studies are required to strengthen the validity of this strategy.

Disclosure statement

No potential conflict of interest was reported by the author(s).

Funding

This research has been supported by the Ministry of Transport of Vietnam Foundation [grant number DT194027].

ORCID

X. K. Dang  <http://orcid.org/0000-0002-5367-3992>

References

- [1] Craig C, Islam M. Integrated power system design for offshore energy vessels and deepwater drilling rigs. *IEEE Trans Ind Appl.* 2012;48(4):1251–1257.
- [2] Dang XK, Do VD, Nguyen XP. Robust adaptive fuzzy control using genetic algorithm for dynamic positioning system. *IEEE Access.* 2020;8:22077–222092.
- [3] Do VD, Dang XK. Fuzzy adaptive interactive algorithm design for marine dynamic positioning system under unexpected impacts of Vietnam Sea. *Indian J Geo-Mar Sci.* 2020;49(11):1764–1771.
- [4] Do VD, Dang XK. Optimal control for torpedo motion based on fuzzy-PSO advantage technical. *Telecommun Comput Electron Control.* 2018;15(4):2999–3007.
- [5] Værnø SA, Skjetne R, Kjerstad K, et al. Comparison of control design models and observers for dynamic positioning of surface vessels. *Control Eng Pract.* 2019;85:235–245.
- [6] Yang H, Deng F, He Y, et al. Robust nonlinear model predictive control for reference tracking of dynamic positioning ships based on nonlinear disturbance observer. *Ocean Eng.* 2020;215:1–9.
- [7] Liang K, Lin X, Chen Y, et al. Adaptive sliding mode output feedback control for dynamic positioning ships with input saturation. *Ocean Eng.* 2020;206:1–17.
- [8] Von Ellenrieder KD. Stable backstepping control of Marine vehicles with actuator rate limits and saturation. *IFAC-PapersOnLine.* 2018;51(29):262–267.
- [9] Sørensen AJ. A survey of dynamic positioning control systems. *Annu Rev Control.* 2011;35(1):123–136.
- [10] Dang XK, Tran TD. Modeling techniques and control strategies for jack-up rig: a state of the art and challenges. *IEEE Access.* 2021;9:155763–155787.
- [11] Wang L, Wu Q, Liu JL, et al. State-of-the-art research on motion control of maritime autonomous surface ships. *J Mar Sci Eng.* 2019;7(12):438–470.
- [12] Sun Y, Xu J, Qiang H, et al. Adaptive neural-fuzzy robust position control scheme for Maglev train systems with experimental verification. *IEEE Trans Ind Electr.* 2019;66(11):8589–8599.
- [13] Sun Y, Xu J, Wu H, et al. Deep learning based semi-supervised control for vertical security of Maglev vehicle with guaranteed bounded airgap. *IEEE Trans Intell Transp Syst.* 2021;22(7):4431–4442.
- [14] Benetazzo F, Ippoliti G, Longhi S, et al. Advanced control for fault-tolerant dynamic positioning of an offshore supply vessel. *Ocean Eng.* 2015;106:472–484.
- [15] Gu MX, Pao YH, Yip PPC. Neural-net computing for real-time control of a ship's dynamic positioning at sea. *Control Eng Practice.* 1993;1(2):305–314.
- [16] Xia G, Shi X, Fu M, et al. Design of dynamic positioning systems using hybrid CMAC-based PID controller for a ship. *IEEE International conference mechatronics and automation; Niagara Falls, Canada; 2005 Aug, p. 825–830.*
- [17] Ta VP, Dang XK, et al. Designing dynamic positioning system based on robust recurrent cerebellar model articulation controller. *The 4th International conference on green technology and sustainable development (GTSD); HoChiMinh, Vietnam; 2018 Nov, p. 652–657.*
- [18] Tiwari K, Krishnankutty P. Dynamic positioning of an oceanographic research vessel using fuzzy logic controller in different sea states. *Mar Syst Ocean Technol.* 2021;16 (3): 221–236.
- [19] Tiwari K, Waghmare LM, Krishnankutty P. Single input fuzzy logic controller tuning for steering control of autonomous underwater vehicle: genetic algorithm approach. *Indian control conference; Hyderabad, India; 2016 March, p. 335–340.*
- [20] Wang YL, Han QL, Fei MR, et al. Network-based T–S fuzzy dynamic positioning controller design for unmanned marine vehicles. *IEEE Trans Cyber.* 2018;48 (9):2750–2763.

- [21] Zheng MJ, Yang SH, Li LN. Stability analysis and T-S fuzzy dynamic positioning controller design for autonomous surface Vehicles based on sampled-data control. *IEEE Access*. 2020;8:148193–148202.
- [22] Hu X, Du J, Shi J. Adaptive fuzzy controller design for dynamic positioning system of vessels. *Appl Ocean Res*. 2015;53:46–53.
- [23] Dang XK, Ho L AH, Do VD. Analyzing the sea weather effects to the ship maneuvering in Vietnam's Sea from BinhThuan Province to Ca Mau Province based on fuzzy control method. *Telecommun Comput Electron Control*. 2018;16(2):533–543.
- [24] Liu Y, Guo C, Lei Z. Intelligent control based on ADRC for large container ship course keeping. *Lect Notes Electr Eng*. 2013;254:195–206.
- [25] Guo C, Wang D, Li Y. Modeling and simulation for super large twin-propeller twin-rudder ship and its course ADRC. *Commun Comput Inform Sci*. 2016;644:89–99.
- [26] Fang MC, Lee ZY. Application of neuro-fuzzy algorithm to portable dynamic positioning control system for ships. *Int J Nav Arch Ocean Eng*. 2016;8(1):38–52.
- [27] Lakshmi S, Jitendra RR. Relationship between Kalman and notch filters used in dynamic ship positioning systems. *Electron Lett*. 1978;14(1):399–400.
- [28] Lin X, Nie J, Jiao Y, et al. Nonlinear adaptive fuzzy output-feedback controller design for dynamic positioning system of ships. *Ocean Eng*. 2018;158:186–195.
- [29] Xu R, Zhou M. Sliding mode control with sigmoid function for the motion tracking control of the piezo-actuated stages. *Electron Lett*. 2017;53(2):75–76.
- [30] Salam AO, Sheriff RE, Al-Araji SR, et al. Adaptive interacting multiple model-Kalman filter for multitaper spectrum sensing in cognitive radio. *Electron Lett*. 2018;54(5):321–322.
- [31] Bai G, Meng Y, Liu L, et al. Anti-sideslip path tracking of wheeled mobile robots based on fuzzy model predictive control. *Electron Lett*. 2020;56(10):490–493.
- [32] Ha QP. Robust sliding mode controller with fuzzy tuning. *Electron Lett*. 1996;32(17):1626–1628.
- [33] Choi JY, Kim MS. Robust adaptive control of feedback linearised systems with time-varying disturbances. *Electron Lett*. 1997;33(16):979–986.
- [34] Do VD, Dang XK, et al. Optimized multi-cascade fuzzy model for ship dynamic positioning system based on genetic algorithm. 5th EAI International conference on industrial networks and intelligent systems (INISCOM 2019); HoChiMinh, Vietnam; 2019 Aug, p. 165–181.
- [35] Fossen TI, Strand JP. Passive nonlinear observer design for ships using Lyapunov methods: full-scale experiments with a supply vessel. *Automatica*. 1999;35:3–16.
- [36] Wang Y, Wang H, Li M, et al. Adaptive fuzzy controller design for dynamic positioning ship integrating prescribed performance. *Ocean Eng*. 2021;219:107956–107966.
- [37] Tee KP, Ge SS. Control of fully actuated ocean surface vessels using a class of feedforward approximators. *IEEE Trans Control Syst Technol*. 2006;14(4):750–756.
- [38] Sivalingam R, Chinnamuthu S, Dash SS. A modified whale optimization algorithm-based adaptive fuzzy logic PID controller for load frequency control of autonomous power generation systems. *Automatika*. 2017;58(4):410–421.
- [39] Do VD, Dang XK. The fuzzy particle swarm optimization algorithm design for dynamic positioning system under unexpected impacts. *J Mech Eng Sci*. 2019;13(3):5407–5423.
- [40] Nafia N, El-Kari A, Ayad H, et al. A robust type-2 fuzzy sliding mode controller for disturbed MIMO nonlinear systems with unknown dynamics. *Automatika*. 2018;59(2):194–207.
- [41] Min W, Liu Q. An improved adaptive fuzzy backstepping control for nonlinear mechanical systems with mismatched uncertainties. *Automatika*. 2019;60(1):1–10.
- [42] Zhang T, Ge SS, Hang CC. Stable adaptive control for a class of nonlinear systems using a modified Lyapunov function. *IEEE Trans Autom Control*. 2000;45(1):129–132.
- [43] Wang JQ, Zou ZJ, Wang T. Path following of a surface ship sailing in restricted waters under wind effect using robust guaranteed cost control. *Int J Nav Arch Ocean Eng*. 2019;11(1):606–623.